

# Atomistic details of effect of disulfide bond reduction on active site of Phytase B from *Aspergillus niger*: A MD Study

Kapil Kumar<sup>1</sup>, Mudit Dixit<sup>2</sup>, JM Khire<sup>1</sup> & Sourav Pal<sup>2\*</sup>

<sup>1</sup>NCIM, Biochemical Sciences Division, <sup>2</sup>Electronic Structure Theory Group, Physical Chemistry Division, CSIR-National Chemical Laboratory, Dr. Homi Bhabha Road, Pune 411 008, India; Sourav Pal - Email: s.pal@ncl.res.in; Phone: +9125902600; Fax: +9125902601 \*Corresponding author

Received November 18, 2013; Accepted November 24, 2013; Published December 06, 2013

## Abstract:

The molecular integrity of the active site of phytases from fungi is critical for maintaining phytase function as efficient catalytic machines. In this study, the molecular dynamics (MD) of two monomers of phytase B from *Aspergillus niger*, the disulfide intact monomer (NAP) and a monomer with broken disulfide bonds (RAP), were simulated to explore the conformational basis of the loss of catalytic activity when disulfide bonds are broken. The simulations indicated that the overall secondary and tertiary structures of the two monomers were nearly identical but differed in some crucial secondary-structural elements in the vicinity of the disulfide bonds and catalytic site. Disulfide bonds stabilize the  $\beta$ -sheet that contains residue Arg66 of the active site and destabilize the  $\alpha$ -helix that contains the catalytic residue Asp319. This stabilization and destabilization lead to changes in the shape of the active-site pocket. Functionally important hydrogen bonds and atomic fluctuations in the catalytic pocket change during the RAP simulation. None of the disulfide bonds are in or near the catalytic pocket but are most likely essential for maintaining the native conformation of the catalytic site.

**Keywords:** Phytase B; Active site integrity, Disulfide bonds, Thermostability, Molecular Dynamics Simulations, Protein folding.

**Abbreviations:** PhyB, 2.5 pH acid phosphatase from *Aspergillus niger*; NAP, disulphide intact monomer of Phytase B; RAP, disulphide reduced monomer of Phytase B; Rg, radius of gyration; RMSD, root mean square deviation; MD, molecular dynamics.

## Background:

Phosphorus is an essential nutrient for all life; it is a component of ATP, phospholipids and nucleic acids [1]. Phosphorus is mainly stored as phytate in most foods derived from plants [2]. Phytase (EC 3.1.3.8) hydrolyzes phytate into free phosphorus and lower derivatives of inositol phosphate [3].

Previously phytase B (PhyB) identified as an acid phosphatase, but PhyB was later found to also hydrolyze phytate quite efficiently at pH 2.5 [4]. PhyB from *Aspergillus niger* belongs to the family of histidine acid phosphatases [5]. This PhyB is more

heat-tolerant than other fungal phytases, with optimal activity at 58 °C [6, 7]. Due to its broad pH stability, substrate specificity and suitability to hydrolyze phytate in stomachs under highly acidic conditions, PhyB is a common supplement in animal feed [8, 9].

PhyB is composed of 460 amino acid residues [10]. The structure of PhyB can be subdivided into a large  $\alpha/\beta$ -domain with a twisted six-stranded  $\beta$ -sheet surrounded by several  $\alpha$ -helices, and a small  $\alpha$ -domain. *A. niger* PhyB has five disulfide bonds at positions 52–368, 109–453, 197–422, 206–279 and 394–

402 (Figure 1a). Two (109–453 and 197–422) maintain the ordered C-terminal structure. Most of the disulfide bonds are present in the loops near the surface in the C-terminus. The conserved catalytic residues, including a catalytic motif of 62RHGXRP67 and a substrate-binding motif of 318HD319, are all positioned in the deep crevice at the interface of the large  $\alpha/\beta$ -domain and the small  $\alpha$ -domain (Figure 1b).

An earlier report suggested an essential role for these disulfide bridges in maintaining the native structure of the enzyme and its catalytic activity [11]. Ullah and co-workers reported the significant role of these disulfide bonds in maintaining the native conformation of PhyA and PhyB [12–14]. They also provided experimental evidence that phytase denatured with guanidium hydrochloride could recover activity when the denaturant was diluted into the reaction system in the absence of Tris(2carboxyethyl)phosphine but could not recover activity in the presence of TCEP. The presence of 2 mM TCEP caused around 70% loss in catalytic activity and a 12% decrease in the

hydrodynamic radius [15]. X Wang et al. [16] reported that these disulfide bonds were necessary for the proper folding of PhyA. Conformational changes or relationships between structural changes and biological properties of the enzyme, however, have not been investigated in detail. Such conformational changes in the overall structure and active site of PhyB that occur due to the breakage of all disulfide bonds are of obvious interest.

The dynamics of the active site of phytases from *A. fumigatus* are known, and the roles of the individual residues are established [17, 18]. With the assumption that the catalytic residues of PhyB from *A. niger* follow similar dynamics, we have elucidated the role of disulfide bonds in the integrity of the active site of PhyB by molecular dynamics (MD) simulation. Our results confirm that disulfide bonds play an important role in maintaining the integrity of the active site. We independently simulated fully reduced (RAP) and intact (NAP) PhyB monomers at 300 K for 20 ns.

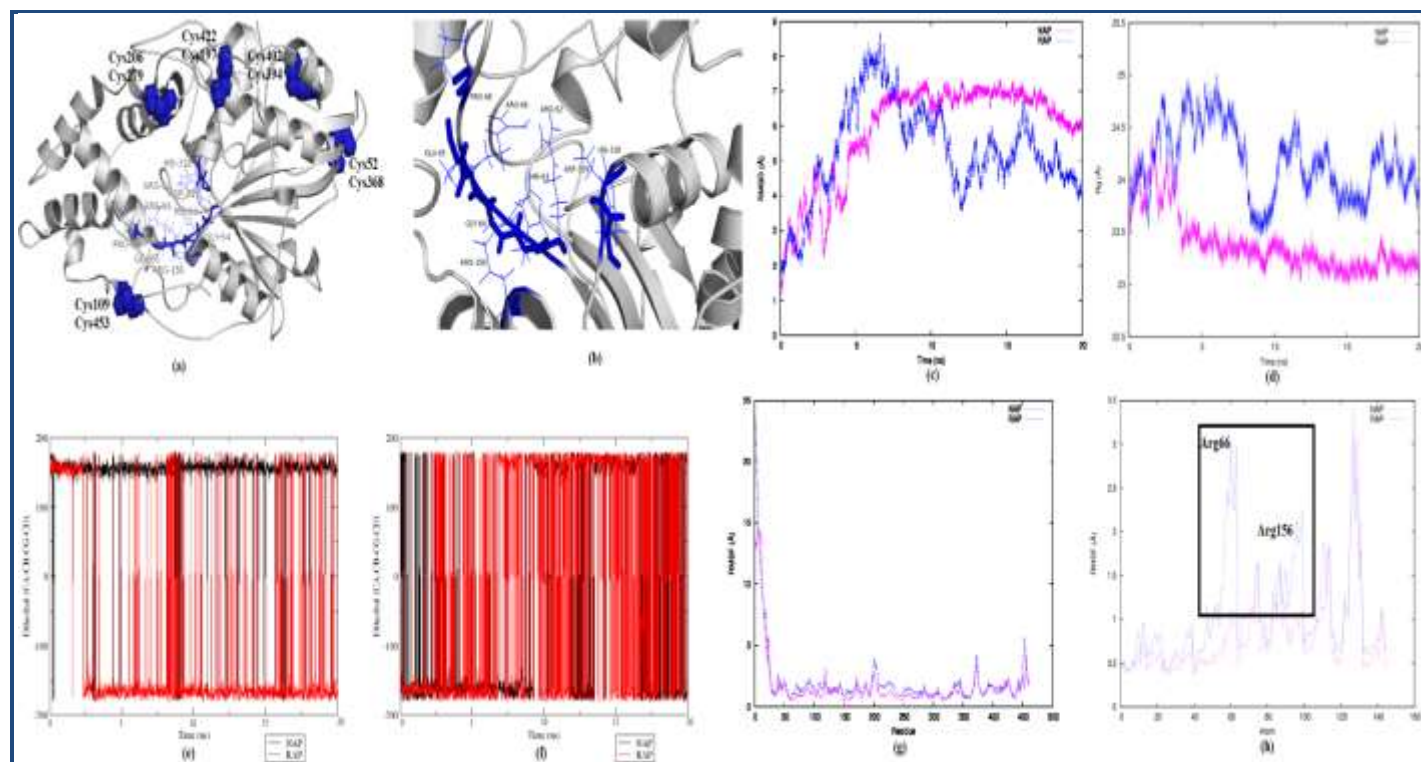


**Figure 1:** (a) Crystal structure of PhyB: positioning of the five disulfide bonds and catalytic residues. (b) Active site residues in the native conformation. (c) Root mean square deviations (RMSDs), (d) Radius of gyration of the C $\alpha$ -atoms. (e) CA-CB-CG-CD Arg66 dihedral angle. (f) CA-CB-CG-CD Arg156 dihedral angle. (g) Root mean square fluctuations (RMSFs) of the C $\alpha$ -atoms. (h) Atomic fluctuations of the active site residues during two 20 ns simulations.

## Methodology:

### Simulation Methods

The crystal structure of *A. niger* PhyB was obtained from the database of the Research Collaboratory for Structural Bioinformatics (RCSB) (PDB ID: 1QFX) [10]. Some residues were missing in the crystal structure; these residues were thus modeled with the Chimera modeling system using 1QFX as the template [19].

### Computation

To investigate the structure in detail, we analyzed a monomer of the dimer. Chain A of PhyB was solvated using the TIP3P

water model [20]. A dodecahedral box was selected to perform MD simulations. PhyB was investigated in the reduced disulfide (RAP) and native (NAP) forms. The system was neutralized by adding sodium and chloride ions. All MD simulations were performed in periodic boundary conditions using the GROMACS (version 4.5.3) software package [21] and the AMBER ff99SB-ILDN force field [22]. The energy of the system was minimized using the steepest descent algorithm for 5000 steps to remove any Van der Waals clashes generated by solvent molecules. An equilibration MD was run for 1 ns to completely mix and equilibrate the contents of the box. Complete mixing and equilibration of the contents were

confirmed by a convergence of potential energy of the system. All MD simulations were performed within NPT (constant number of atoms, pressure and temperature throughout the simulation) ensembles. Temperatures were fixed using the Berendsen temperature coupling algorithm with a coupling constant of 0.1 ps and pressure was kept constant at one bar with a coupling constant of 0.5 ps [23]. The SHAKE algorithm was used to constrain all bond lengths [24, 25]. The Particle Mesh Ewald (PME) method was used to model non-bonded electrostatic and LJ interactions. NPT simulations were performed at 300 K to study the effect of temperature. The total production run of MD simulations was 40 ns including 20 ns simulations of RAP and NAP at 300 K.

## Analysis

All analysis used the GROMACS package. VMD was used for visualization [25]. Secondary structures were calculated using STRIDE [26]. Prior to calculation of the atomic positional fluctuations, we removed the overall translational and rotational motions by superimposing the C $\alpha$ -atoms of each snapshot structure onto those ones of the starting structure of the trajectory, using the least-squares fitting method. Hydrogen bonds were analyzed at a distance of 3 Å and a cut-off angle of 120°.

## Results & Discussion:

### Structural properties

The root mean square deviations (RMSDs) of the backbone  $\alpha$ -carbon atoms of PhyB relative to those in the first snapshot of the trajectories were calculated for both MD simulations (Figure 1c). In NAP, the RMSD of the initial structure was nearly steady around 6 Å. The RMSD of RAP began to depart from that of NAP after 3 ns of simulation and remained slightly lower than the NAP RMSD. Both simulations were thus performed using the same starting structure obtained from 1QFX. The difference in RMSDs indicated that structural changes beginning after 3 ns were due to breakage of the disulfide bonds. The radius of gyration remained unaltered in both simulations (Figure 1d). Reduction of the disulfide bonds thus did not show the expansion of the overall structure of PhyB. These results agreed well with those of Mullaney and Ullah [11].

The overall secondary structure of RAP did not change significantly, but some of the helices were shortened, and some 3/10 helices were lost in the last 1 ns of the simulation. Based on the assignment of secondary structure Table 1 (see supplementary material), using STRIDE [27], a helix from residues 262 to 280 lost six residues which were converted into a turn due to the breakage of the Cys206-Cys279 disulfide bond. The other helix from residues 124 to 134 was lengthened by four residues by the breakage of the Cys109-Cys453 disulfide bond. Some of the 3/10 helices were completely lost in RAP: from residues 256 to 258, 351 to 353 and 434 to 436 Table 2 (see supplementary material). These 3/10 helices were in close proximity to disulfide bonds. The catalytic residue Asp319 moved from the  $\alpha$ -helix to the 3/10 helix, which produced a stable structure. The secondary-structural assignments of the other residues of the catalytic site remained unchanged. Due to these small changes in secondary-structural assignments, the rigidity of the catalytic site was lost in RAP. The structures were fairly compact in both NAP and RAP, which had nearly the same order of secondary and tertiary structure regardless of

changes in the  $\alpha$  and 3/10 helices. The disulfide bonds thus enhanced the global stability of PhyB.

### Hydrogen bonding

We also compared H-bond occupancies during the simulation of two trajectories Table 3 (see supplementary material). Apart from the changes in the pattern of H-bonds of the backbone due to alterations in secondary structure, the occupancy of some functionally important H-bonds in the catalytic motif had notably changed due to the breakage of the disulfide bonds.

The occupancy of the H-bond between the Arg156 and the His63 side chains decreased from 82.71% in NAP to 25.19% in RAP. This H-bond is important for the binding of phytate in the catalytic pocket, and its breakage can greatly affect binding affinity [16, 17]. The H-bond between the side chains of catalytic residues Arg156 and Asn114, which had occupancy of 100% in NAP, was completely lost in RAP. The occupancy of the H-bond between the side chains of Arg156 and Glu114 was reduced from 91.75% to 23.39% in RAP. The change in the pattern of H-bonding allowed more flexibility in the orientation of the side chain of the other binding residue, Arg66. In NAP, the Arg66 side chain was bonded to the side chain of Ser69 with an 88.71% occupancy, which was reduced to 10% in RAP. The side chain of Arg66 became highly flexible with the breakage of this H-bond, reducing the conformational space for the binding of the substrate and thus affecting the catalytic activity of the enzyme. The occupancy of the H-bond between the Arg66 main chain and the Asn249 side chain changed from 61% to 7.55% in RAP.

The changes in the H-bond occupancies of the active site Arg66 and Arg156 side chains reduced rigidity. This loss of rigidity was ultimately due to the breakage of disulfide bonds, which was the main reason for the loss of more than 70% of catalytic activity. The Arg66 and Arg156 side chains lost some of the restrictive factors that were important for their spatial orientations in the catalytic motif and started to rotate after 2.5 ns (Figure 1e). The lower amount of H-bonding in the side chains of Arg66 and Arg156 destabilized the catalytic Arg66 and Arg156 side chains (Figure 1f).

### Dynamic changes

Fig. 4a shows the root mean square fluctuations (RMSFs) in the simulated structures. The RMSF values of residues near disulfide bonds changed significantly, but the overall fluctuations of all cysteines did not change (Figure 1g). The larger effect on the fluctuations of neighboring flexible regions than on the rigid sites of the cysteine residues themselves is in agreement with the results of previous studies on the scorpion toxin and cutinase [27, 28]. The major changes in overall fluctuations occurred in the active-site residues Arg66 and Arg156 (Figure 1h). These two residues have rigid side-chain orientations for allowing productive interactions with the substrate. As previously reported, the binding of phytate to phytase seems not to require main-chain interactions but only side-chain interactions [16, 17]. The Arg66 and Arg156 side chains play important roles in binding of the substrate, formation of the phospho-histidine intermediate and release of the product [16]. Our simulations showed that atomic fluctuations in Arg66 and Arg156 increased drastically after the disulfide bonds were broken.

The distances between atoms His63NE2 and Asp319OD1 and between His63NE2 and Asp319OD2 changed **Table 4** (see **supplementary material**). The distance between His63NE2 and Asp319OD1 is very important for catalysis of the substrate, as proposed in a previous study on *A. fumigatus* phytase [16]. The increase in flexibility after reduction of the disulfide bonds led to these alterations in the distances between the side-chain atoms. As anticipated in the enzymatic dynamics of *A. fumigatus* phytase [17], the catalytic Asp319 binds to two phosphate atoms simultaneously, so these distances are very important for binding and catalysis. Assuming that PhyB follows similar dynamics, our results suggest that the loss of PhyB activity is a conformational consequence of broken disulfide bonds.

## Conclusion:

The reduction of disulfide bonds alters the functionally essential network of H-bonds, the distances between atoms and the dihedral angles in the active-site residues of PhyB. The catalytically important distance between atom His63NE2 and atom Asp319OD1 is increased, indicating an abnormal interaction between the phosphate ion and these two residues. Arg66 and Arg156 help to stabilize the phospho-histidine intermediate and the release of the product. Changes in the mobility of the side-chains of these residues would likely lead to the loss of activity. Our results thus provide a possible mechanism for the loss of catalytic activity after the breakage of disulfide bonds.

## Acknowledgement:

We acknowledge the Centre of Excellence in Advanced Computing, National Chemical Laboratory, Pune, for providing computational facilities. M Dixit and K Kumar acknowledge University Grant Commission for senior research fellowships. SP acknowledges the Shanti Swarup Bhatnagar and JC Bose fellowships toward the completion of this work.

## References:

- [1] Harland BF & Morris ER, *Nutrition Research*. 1995 **15**: 733  
 [2] Reddy NR *et al. Adv Food Res*. 1982 **28**: 1 [PMID: 6299067]  
 [3] Mitchell D *et al. Microbiology*. 1997 **143**: 245 [PMID: 9025298]

- [4] Ullah AHJ & Cummins BJ, *Prep Biochem*. 1997 **17**: 397 [PMID: 3438253]  
 [5] Vincent JB *et al. Trends Biochem Sci*. 1992 **17**: 105 [PMID: 1412693]  
 [6] Ullah AHJ & Gibson DM, *Prep Biochem*. 1987 **17**: 63 [PMID: 3035533]  
 [7] Wyss M *et al. Appl Environ Microbiol*. 1998 **64**: 4446 [PMID: 9797305]  
 [8] Ullah AHJ *et al. J Agric Food Chem*. 1994 **42**: 423  
 [9] Soni SK *et al. World J Microbiol Biotechnol*. 2010 **26**: 2009 [PMID: 20976287]  
 [10] Kostrewa D *et al. J Mol Biol*. 1999 **288**: 965 [PMID: 10329192]  
 [11] Ullah AH *et al. J Agric Food Chem*. 2008 **56**: 8179 [PMID: 18683944]  
 [12] Ullah AH & Mullaney EJ, *Biochem Biophys Res Commun*. 1996 **227**: 311 [PMID: 8878514]  
 [13] Ullah AHJ *et al. Biochem Biophys Research Comm*. 2005 **327**: 993 [PMID: 15652493]  
 [14] Mullaney EJ & Ullah AH, *Biophys Res Commun*. 2005 **328**: 404 [PMID: 15694362]  
 [15] Wang X *et al. Biochem Cell Biol*. 2004 **82**: 329 [PMID: 15060628]  
 [16] Liu Q *et al. Structure*. 2004 **12**: 1575 [PMID:15341723]  
 [17] Xiang T *et al. J Mol Biol*. 2004 **339**: 437 [PMID: 15136045]  
 [18] Pettersen EF *et al. J Comput Chem*. 2004 **13**: 1605 [PMID: 15264254]  
 [19] Jorgensen WL *et al. J Chem Phys*. 1983 **79**: 926  
 [20] Hess B *et al. J Chem Theory Comput*. 2008 **44**: 35  
 [21] Lindorff-Larsen K *et al. Proteins*. 2010 **78**: 1950 [PMID: 20408171]  
 [22] Berendsen HJC *et al. J Chem Phys*. 1984 **81**: 3684  
 [23] Ryckaert JP *et al. J Comp Phys*. 1977 **23**: 327  
 [24] Miyamoto S *et al. J Comput Chem*. 1992 **13**: 952  
 [25] Humphrey W *et al. J Molec Graphics*. 1996 **14**: 33 [PMID: 8744570]  
 [26] Heinig M *et al. Nucleic Acids Res*. 2004 **32**: W500 [PMID: 15215436]  
 [27] Moghaddam ME *et al. Proteins*. 2006 **1**: 188 [PMID: 16400645]  
 [28] Matak MY *et al. Biochem Biophys Res Comm*. 2009 **390**: 201 [PMID: 19781526]

Edited by P Kanguane

Citation: Kumar *et al.* Bioinformation 9(19): 963-967 (2013)

**License statement:** This is an open-access article, which permits unrestricted use, distribution, and reproduction in any medium, for non-commercial purposes, provided the original author and source are credited

## Supplementary material:

**Table 1:** STRIDE secondary-structural assignment.

Residues	NAP	RAP
124-134 ( $\alpha$ -Helix)	124-134	123-137
262-280 ( $\alpha$ -Helix)	262-280	262-174

**Table 2:** STRIDE secondary-structural assignment of the lost or changed secondary structures.

Residues	NAP	RAP
256-258	3/10 Helix	Turn
351-353	3/10 Helix	Turn
371	Turn	B-Bridge
374	Turn	B-Bridge
434-436	3/10 Helix	Turn
319-321	$\alpha$ -Helix	3/10 Helix

**Table 3:** Hydrogen-bond occupancy between donor and acceptor atoms of active-site residues during 20 ns NAP and RAP simulations

Donor	Acceptor	NAP (%)	RAP (%)
Arg156 Side chain	His63 Side chain	82.71	25.19
Arg156 Side chain	Glu114 Side chain	91.75	23.39
Arg156 Side chain	Asn112 Side chain	100	-
Arg66 Main chain	Asn249 Side chain	61.02	7.55
Arg66 Side chain	Ser69 Side chain	88.71	10.09

**Table 4:** Distances in angstroms between functional atoms of active-site residues in the last 1 ns of the NAP and RAP simulations

Atom 1	Atom 2	NAP	RAP
His63NE2	Asp319OD1	4.5	7.5
His63NE2	Asp319OD2	7.1	6.2
Asp319OD2	Arg66NH1	9.15	13.2
Arg156NH2	His318ND1	7.25	10.5